Walter, J., *et al.*: Experimental Investigation Of An Annular Diffuser For Axial Flow Fan…
THERMAL SCIENCE, Year 2016, Vol. 20, Suppl. 6, pp. S1-S14

S1

EXPERIMENTAL INVESTIGATION OF AN ANNULAR DIFFUSER FOR AXIAL FLOW FAN CONFIGURATIONS AT DIFFERENT INFLOW PROFILES

by

Johannes WALTER[a], Dieter WURZ[b], Stefan HARTIG[b], and Martin GABI[a]*

[a]Institute of Fluid Machinery, Karlsruhe Institute of Technology (KIT), 76131 Karlsruhe, Germany

[b]ESGmbH, Emissionsmesstechnik und Strömungsmechanik, 76532 Baden-Baden, Germany

Axial fans are used in power plants for fresh air supply and flue gas transport. A typical configuration consists of an axial fan and annular diffuser which connects the fan to the following piping. In order to achieve a high efficiency of the configuration not only the components have to be optimized but also their interaction. The present study focuses on the diffuser of the configuration. Experiments are performed on a diffuser-piping configuration in order to investigate the influence of the velocity profile of the fan outlet on the pressure recovery of the configuration. Two different diffuser inlet profiles are generated, a homogeneous profile and a profile with the typical outlet characteristics of a fan. The latter is generated by the superposition of screens in the inlet zone. The tests are conducted at a high Reynolds number ($Re \approx 4 \cdot 10^5$). Mean velocity profiles and wall shear stresses are measured with hydraulic methods (Prandtl and Preston tubes). The results show that there is a lack of momentum at the outer wall of the diffuser and high shear stresses at the inner wall in case of the homogeneous inflow profile. For the typical fan outlet profile it can be shown that there is an opposite effect with high wall shear stresses at the outer wall while the boundary layer of the inner wall lacks momentum. The pressure recovery of the configuration is in good agreement with previous studies.

Key words: *annular diffuser, flow separation, fan outflow profile, Preston method, pressure recovery*

Introduction

Depending on the application of a fan, a large part of the total pressure increase is available as dynamic pressure at the fan outlet. Annular diffusers are used to reduce the dynamic pressure downstream the impeller of the axial fan. Figure 1 shows a common fan-diffuser configuration in a large-scale plant. In order to achieve a high efficiency of the configuration the dynamic pressure needs to be converted into a static pressure increase. Depending on the operation point of the fan, the outlet profile of fan respectively the inlet profile at the annular diffuser changes and affects the diffuser efficiency. The goal of this

_____

* Corresponding author; e-mail: walter@kit.edu

study is to determine the pressure recovery coefficient cp of the configuration for different inflow profiles.
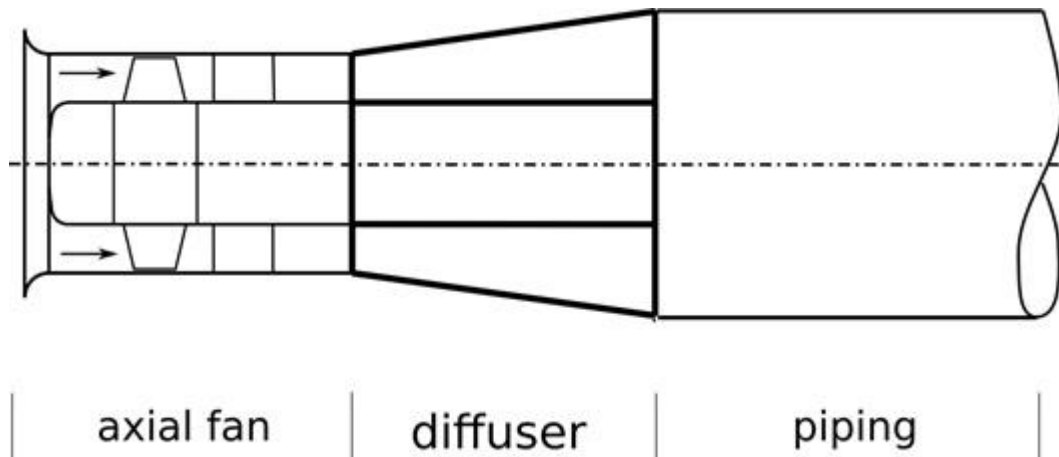
Figure 1. State of art fan-diffuser configuration

Annular diffusers are investigated in several studies. The most notable work was performed by Sovran and Klomp [1]. They investigated pressure recovery for different diffuser length and area ratios for an inflow profile with low aerodynamic blockage B. Their generated diffuser performance chart is commonly used as a guideline for diffuser construction. Stevens and Williams [2] examined the performance of two annular diffuser configurations. They performed their experiments for a uniform inlet profile, a fully developed profile and increased turbulent mixing. According to their research the inlet profile and the turbulence intensity have a strong impact on the overall pressure recovery. In 1982, Dierksen published datasets of velocity profiles in annular diffusers measured by Laser Doppler Velocimetry [3]. Japikse published a study on the influence of geometry, swirl and blockage on annular diffuser performance [4]. He derived a correlation based on measurements to estimate diffuser performance.

Understanding the effect of the fan outflow profile on the diffuser performance is necessary to improve the performance of fan-diffuser-piping configurations. In the present study, a fan outflow profile is reproduced and the diffuser flow characteristics are analysed. The results are compared to the flow characteristics of the diffuser with undisturbed inflow. In order to achieve realistic reference data at the diffuser inlet, in-situ profile measurements at the outlet of an axial fan in a coal-fired power plant are used as reference. Besides velocity profiles and pressure recovery, a closer look is taken on the wall shear stress distribution in the diffuser and downstream to characterize flow stability. A test rig is constructed and set up in the laboratories. The annular diffuser is designed according to state of art diffusers in power plants at laboratory scale. The geometry of the diffuser is chosen according to the guideline of Sovran and Klomp (Figure 2). By means of their chart the maximum possible pressure recovery cp for a given diffuser length (cp*) can be determined. A pressure recovery $cp = 0.59$ is expected for the investigated diffuser according to their chart.

Walter, J., *et al.*: Experimental Investigation Of An Annular Diffuser For Axial Flow Fan…
THERMAL SCIENCE, Year 2016, Vol. 20, Suppl. 6, pp. S1-S14

S3
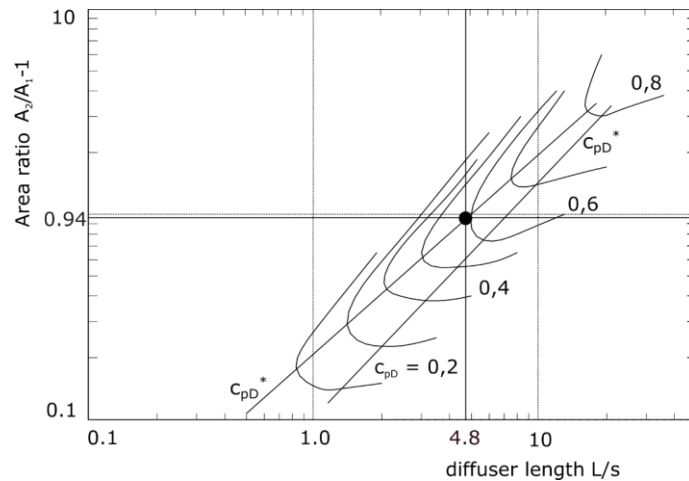
Figure 2. Diffuser Performance Chart (Sovran and Klomp [1])

Experimental apparatus and methods

The test rig is shown in figure 3. A filter is installed in front of the inlet nozzle to homogenize the inflow and keep the airflow clean. The entry section ensures the laminar to turbulent transition of the boundary layer. The test rig is designed to conduct experiments for different inflow profiles, therefore an installation section for screens is arranged 1.5s upstream the annular diffuser. The housing of the diffuser is conical. The hub, which is installed in the center, is cylindrical and aligned by radial struts at the inlet and the outlet of the diffuser. Downstream the hub the annular diffuser is connected to a cylindrical pipe. The hub ends with the beginning of the pipe. This installation is followed by a plenum chamber and a radial fan. The opening angle of the annular diffuser is $\alpha/2=7.2°$. The test rig is constructed by sheet metal with a high standard accuracy (accuracy of laser cutting machine for manufacturing: -+0.05mm).
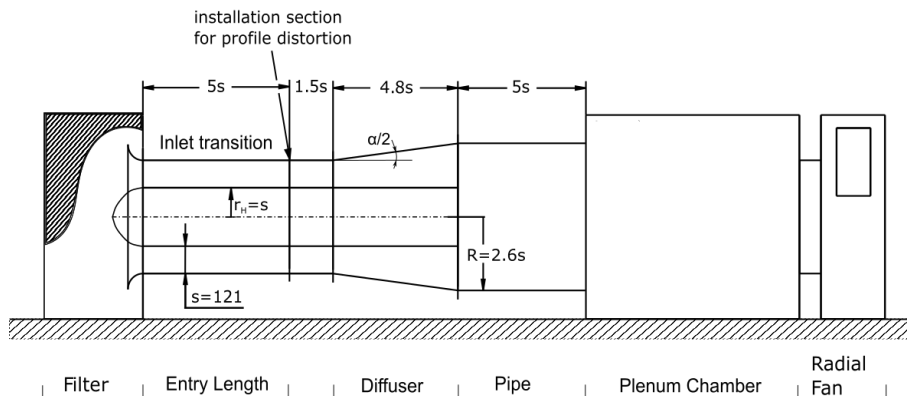
Figure 3. Diffuser Performance Chart (Sovran and Klomp [1])

In the present study, two different diffuser inlet profiles are analysed. An undisturbed profile and a typical axial fan outflow profile. Figure 4 shows the mean axial velocity profiles c_{ax} at diffuser inlet. The profiles are averaged in circumferential direction (4 axes). The reference fan outflow profile (Figure 4: Diffuser inflow profiles (left: undisturbed inlet profile, right: reconstructed fan profile), right) is measured at a power plant fan working at nominal load. The investigated fan is equipped with guide vanes downstream the impeller of the fan to remove the swirl in the flow. The velocity profile shows a maximum at the outer region of the annular gap ($s_i/s \approx 0.75$). Due to harsh measurement conditions in the plant, the boundary layers could not be resolved. The fan outflow profile is reconstructed at the inlet of the test rig diffuser by the superposition of two screens (Figure 5: Screens for inflow disturbance). The screens are mounted in the installation section upstream the annular diffuser of the rig.
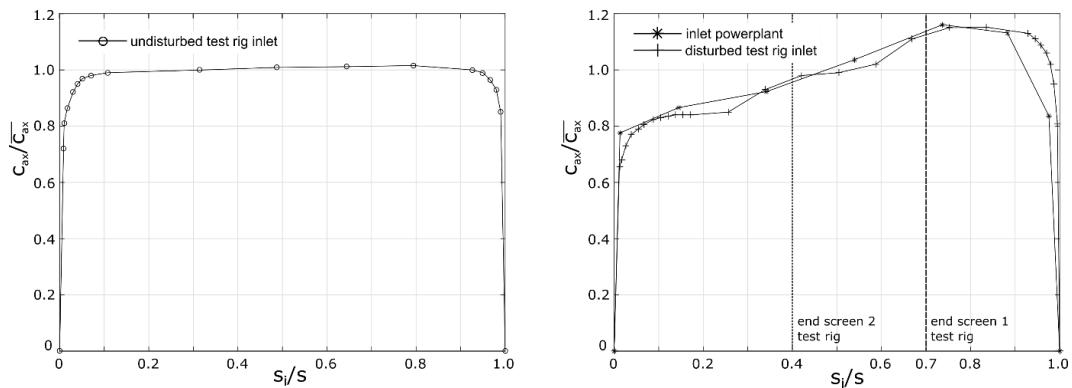
Figure 4. Diffuser inflow profiles (left: undisturbed inlet profile, right: reconstructed fan profile)

According to Traupel [5] a Reynolds independence of the diffuser flow is achieved at Reynolds Numbers Re $>1 \cdot 10^5$ and Mach Numbers Ma<0.7. In the present study experiments are performed at Re$\approx 4 \cdot 10^5$ and Ma≈ 0.1.

Figure 5. Screens for inflow disturbance

Walter, J., *et al.*: Experimental Investigation Of An Annular Diffuser For Axial Flow Fan…
THERMAL SCIENCE, Year 2016, Vol. 20, Suppl. 6, pp. S1-S14

S5
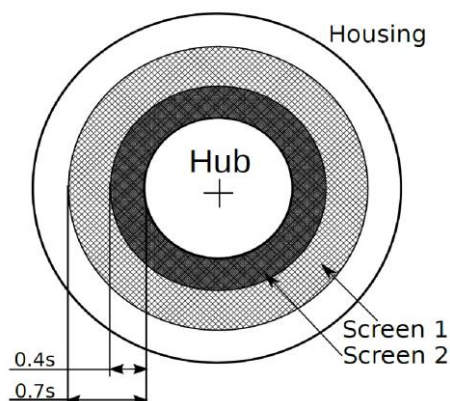
Measurement technique

The velocity profiles are measured by a Prandtl probe and a MKS Baratron pressure converter. An integration time of 10 s is used for averaging. A boundary layer displacement correction according to Mc-Millan is applied, the correction can be found in [6]. The wall shear stress is determined by an extended Preston method CPM3 [7]. This method is based on he extended law of the wall according to Szablewski (1), which considers an adverse pressure gradient.

$$u^+ = \int_0^{y^+} \frac{2(1+p^+y^+)}{1+\sqrt{1+4(ky^+)^2(1+p^+y^+)(1-\exp\left(\frac{y^+}{A^+}\sqrt{1+p^+y^+}\right))^2}}dy^+ \tag{1}$$

$$u^+ = \frac{u}{u_\tau} \tag{2}$$

$$y^+ = \frac{uy}{\nu} \tag{3}$$

$$p^+ = \frac{\nu}{\rho u_\tau^3 \nu}\frac{dp}{dx} \tag{4}$$

The parameters κ, A^+, p^+ have to be determined to find the local law of the wall. Near wall velocity measurements are conducted with pressure probes. The law of the wall (1) is transferred in its dimensional formulation using the friction velocity u_τ. A parameter variation of u_τ, κ, A^+, p^+ is performed until an appropriate fit of measured near wall profile and law of the wall is found. For more detailed information refer the study of Nitsche "A computational Preston tube method" [7]. The turbulence intensity Tu is measured at the diffuser inlet, therefore a 1-D single wire Dantec Streamline hot wire anemometry system is used.

Measurement sections

Velocity profile measurements are conducted at diffuser inlet (MP1) and outlet (MP4) at four axes (0°, 90°, 180°, 270°) and at MP2 and MP3 at one axis (0°). The turbulence intensity Tu is recorded at diffuser inlet (MP1, 0°). The wall shear stress τ_{Wall} and the near wall velocity profiles are measured at MP1, MP2, MP3, and MP4 at one circumferential position (0°).
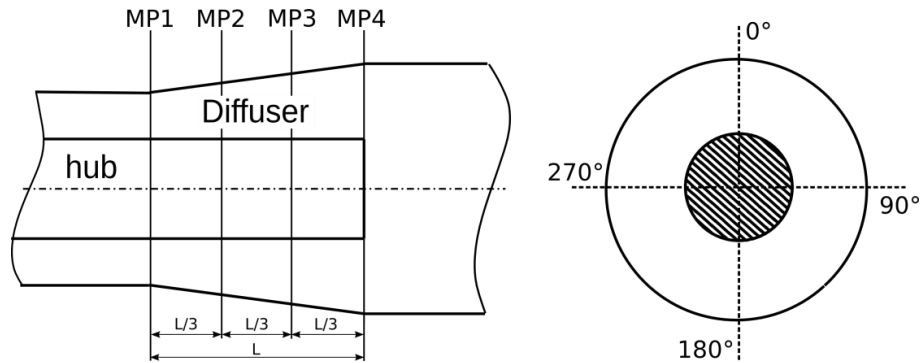
Figure 6. Measurement sections

Results and Discussion

The inlet conditions in the diffuser are described in Table 1. The mean turbulence intensity (Tu) at the inlet of the undisturbed inflow configuration is Tu = 5.4% and in the disturbed configuration is Tu = 5.7%. In both configurations, a Reynolds independency is expected (Re > 1·10^5). In order to quantify the blockage of the profile at the inlet the aerodynamic blockage B (5) is introduced analog to [1, 4].

$$B = 1 - \frac{1}{A} \int \frac{c_{ax}}{c_{ax,\max}} dA \tag{5}$$

Table 1. Inflow conditions to the diffuser

Configuration	$C_{ax,inlet}$ [m/s]	$Re_{hyd,inlet}$ [-]	Tu_{inlet} [%]	B
Undisturbed profile	24.2	3.9×10^5	5.4	0.055
Disturbed profile	24.8	4.0×10^5	5.7	0.17

Flow Measurement in the annular diffuser

Figure 7 shows the development of the velocity profile in the diffuser. The strong dependence of the diffuser outflow profile on the inflow characteristic is visible. As can be seen the undisturbed profile develops a velocity maximum close to the hub. The velocity maximum of the disturbed inlet profile is in the outer region of the annular gap and it is amplified downstream the diffuser. Flow separation is detected at the hub of the diffuser outlet for this configuration. In order to quantify the flow homogeneity the distortion parameter D (6) is introduced [8]. If the parameter D equals zero the flow profile is uniform, a parameter D = 0.2 corresponds to a parabolic profile in a plane channel.

$$D = \left[\frac{A}{\dot{V}^2} \int_{r_i}^{r_o} c_{ax}^2 dA \right] - 1 \tag{6}$$

As can be seen in Figure 8 the distortion D grows strongly monotonous in the diffuser for the undisturbed inflow. A level of D = 0.1 is reached at the diffuser outlet. The disturbed inflow

Walter, J., *et al.*: Experimental Investigation Of An Annular Diffuser For Axial Flow Fan…
THERMAL SCIENCE, Year 2016, Vol. 20, Suppl. 6, pp. S1-S14

S7

starts at $D = 0.03$ and reaches its maximum at $x/L = 2/3$ with $D = 0.15$. Downstream the distortion decreases slightly ($D = 0.14$ at diffuser outlet).
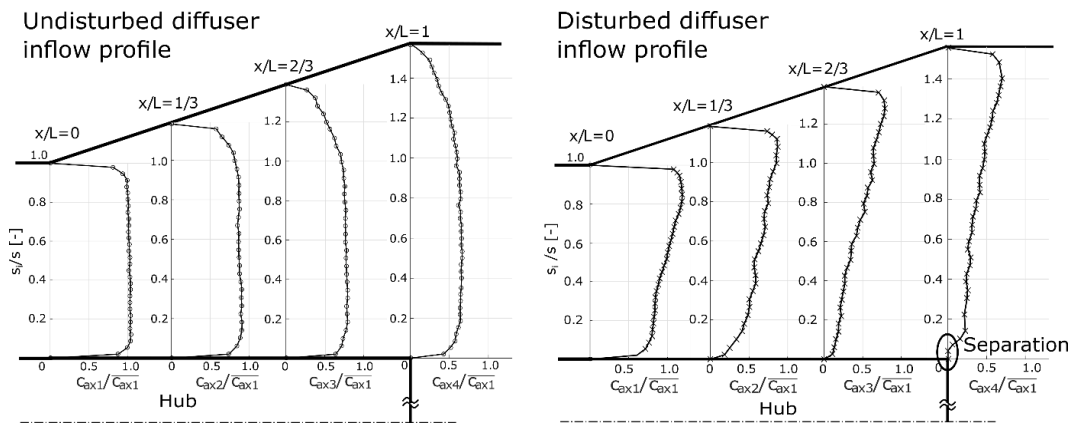
Figure 7. Velocity profiles in the annular diffuser (left: undisturbed inflow, right: disturbed inflow)
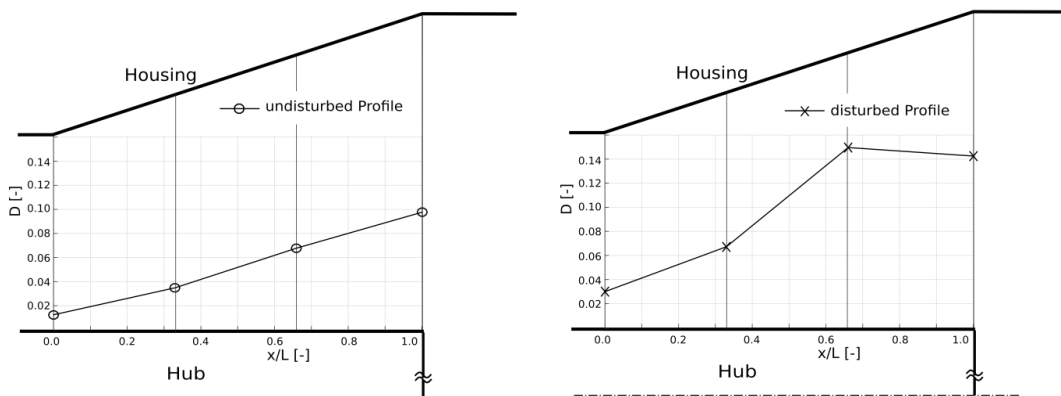
Figure 8. Profile distortion D of the flow (left: undisturbed inflow, right: disturbed inflow)

In order to take a closer look on the flow stability in the annular diffuser, the wall shear stress is analysed at the hub and the housing of the diffuser, therefore the CPM3 Method is used. The CPM3 gives the wall shear stress and the law of the wall. In Figure 9 and Figure 10, the law of the wall and near wall velocity measurements are plotted. As can be seen there is a good agreement of measurement points and the law of the wall.

The undisturbed and disturbed inflow profiles follow the law of the wall ($\kappa = 0.4$, $A^+ = 26$) in the near wall region at the hub and housing. At diffuser outlet the pressure increase has to be considered. The best fit for the extended law of the wall is found for $p^+ = 0.02$ at the hub and $p^+ = 0.04$ at the housing (undisturbed inflow profile). The study of the disturbed profile shows a good fit for $p^+ = 0.04$ at the housing of the diffuser outlet. At the hub wall shear stress cannot be determined due to flow separation.
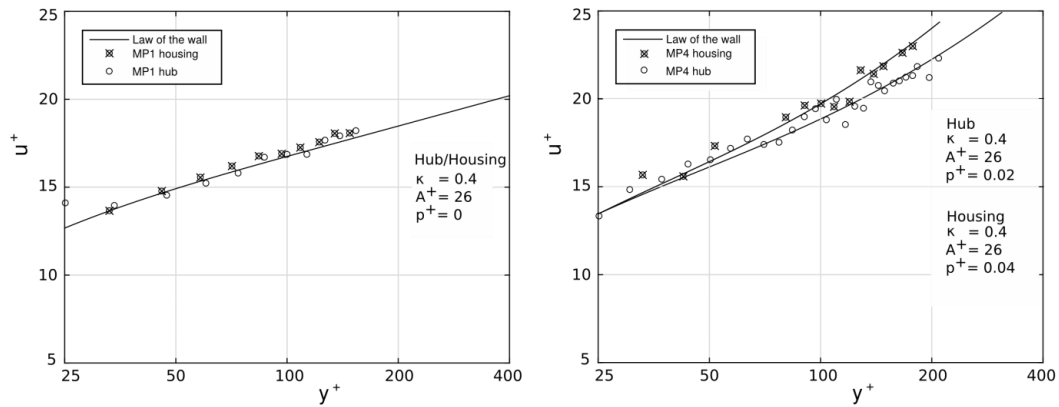
Figure 9. Near wall velocity profiles for undisturbed inflow (left: diffuser inlet, right: diffuser outlet)
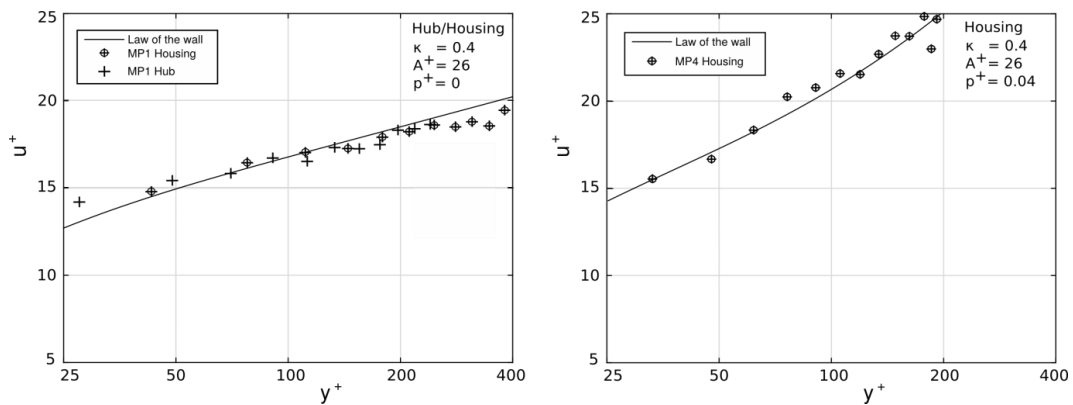
Figure 10. Near wall velocity profiles for disturbed inflow (left: diffuser inlet, right: diffuser outlet)

Next, the flow stability is considered. In literature different parameters indicating a stable forward flow are discussed [9]. In this study a simple approach is chosen. It is assumed that the wall shear stress of a flat plate at corresponding outer flow velocity and distance indicates a stable forward flow. The measured wall shear stress of the diffuser flow is related to the theoretical wall shear stress of a flat plate. In this study a formulation according to Schlichting [10] is used to calculate the wall shear stress along a plate.

$$\tau_{Wall} = \frac{1}{2} \rho c_f u_\infty^2 \tag{7}$$

$$c_f = (2\log_{10}(\text{Re}_x) - 0.65)^{-2.3} \tag{8}$$

Figure 11 shows the wall shear stress distribution along the hub and the housing for both inflow conditions. The wall shear stress at the inlet of the undisturbed inflow configuration is close to the shear stress of a flat plate, while at the diffuser outlet the shear stress decreases at

Walter, J., *et al.*: Experimental Investigation Of An Annular Diffuser For Axial Flow Fan…
THERMAL SCIENCE, Year 2016, Vol. 20, Suppl. 6, pp. S1-S14

S9

the hub to 76 % and at the housing to 51% of the corresponding stress of a flat plate. The wall shear stress at the housing of the disturbed inflow configuration is 1.4 times higher than the corresponding stress of a flat plate. In the diffuser this maximum value decreases to a local minimum of 1.12 at 2/3 of the diffuser length and rises again to 1.19 at the diffuser outlet. The wall shear stress at the hub starts at 0.75 at diffuser inlet and decreases in mean flow direction resulting in flow separation close to diffuser outlet.
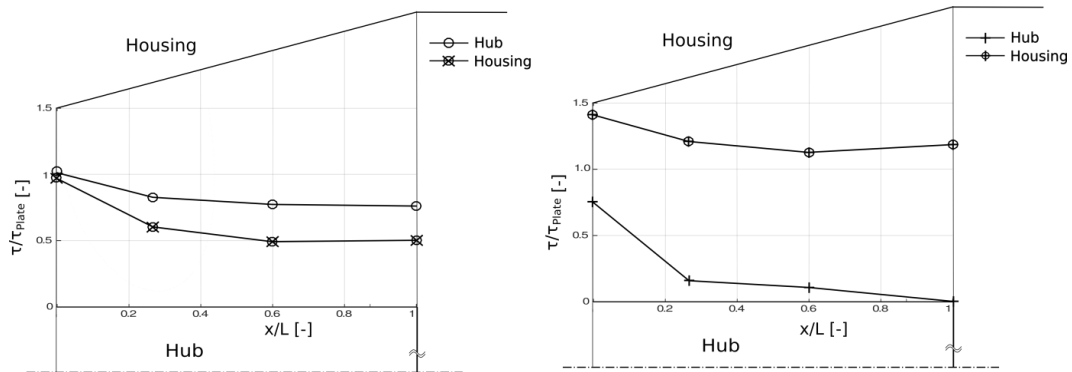
Figure 11. Wall shear stress distribution in the annular diffuser (left: undisturbed inflow, right: disturbed inflow)

Flow Measurement downstream the annular diffuser

The flow downstream the annular diffuser is investigated. At the outlet of the annular diffuser, the hub ends. The sudden increase of area causes a wake area downstream the hub (Figure 12). Figure 12 shows the flow profiles downstream the diffuser. As can be seen the wake area is filled for both configurations at $x/s = 3$. At $x/s = 1.5$ both configurations reach a similar level of homogeneity $D \approx 0.8$ (Figure 13).
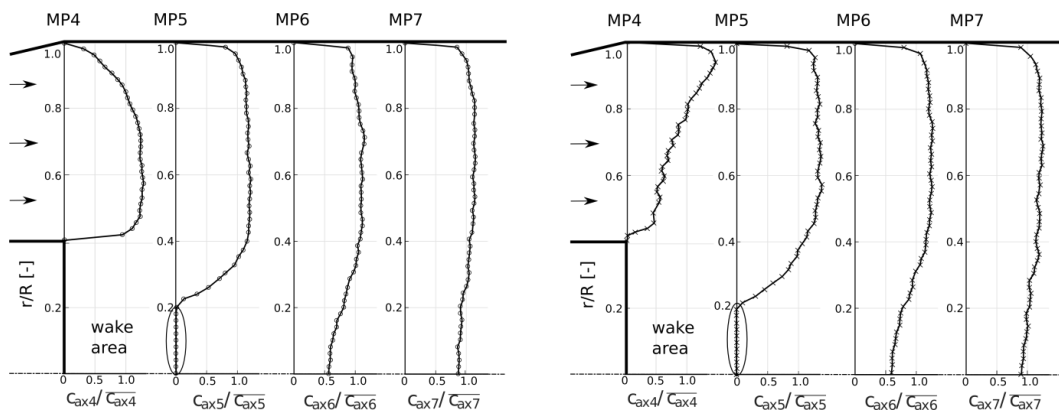
Figure 12. Velocity profile downstream the hub (left: undisturbed inflow, right: disturbed inflow)
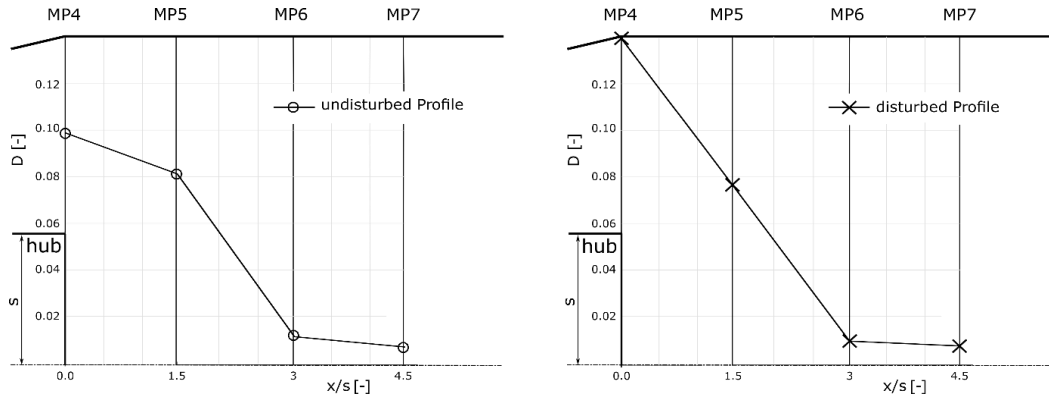
Figure 13. Flow distortion downstream the hub (left: undisturbed inflow, right: disturbed inflow)

The near wall velocity profiles and the law of the wall are plotted at different axial positions. The best agreement is reached at MP7 where the effect of the wake area of the hub nearly vanishes.
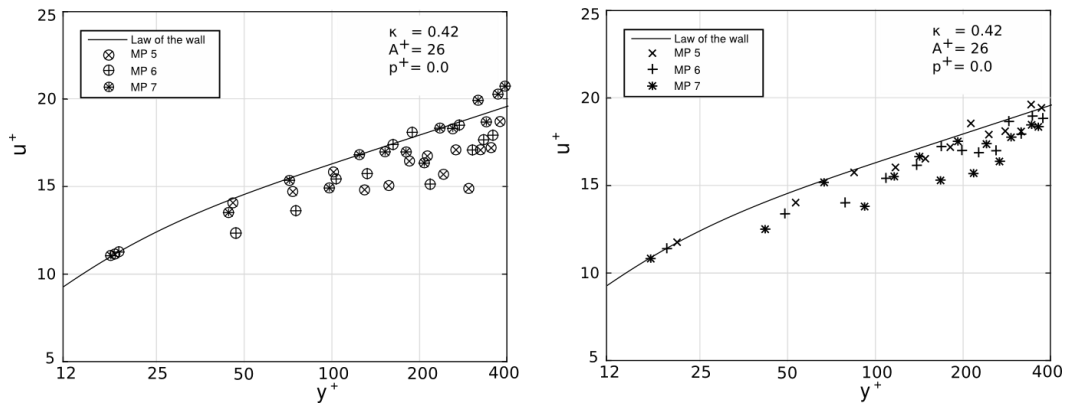
Figure 14. Near wall velocity profiles downstream the hub (left: undisturbed inflow, right: disturbed inflow)

Downstream the hub the wall shear stress at the housing rises. The shear stress maximum is reached at MP6 for the undisturbed inflow and at MP5 for the disturbed inflow. Further downstream the wall shear stress decreases again.

Walter, J., *et al.*: Experimental Investigation Of An Annular Diffuser For Axial Flow Fan…
THERMAL SCIENCE, Year 2016, Vol. 20, Suppl. 6, pp. S1-S14

S11
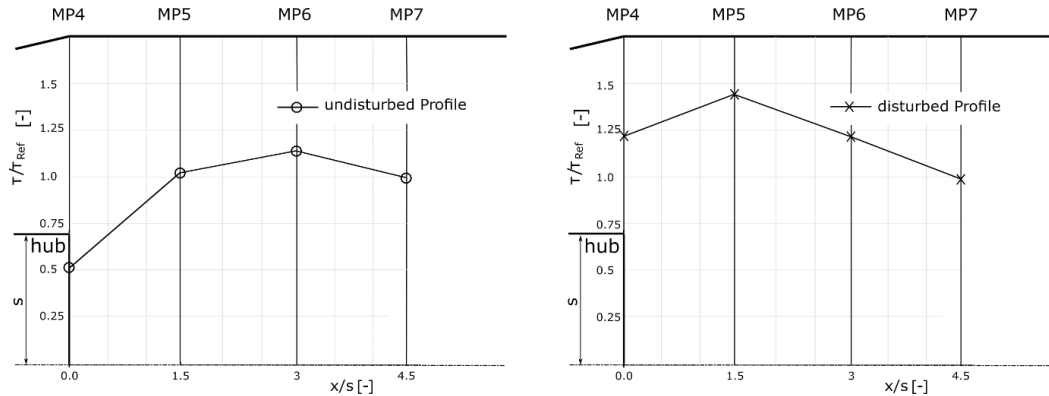
Figure 15. Wall shear stress downstream the hub at the housing of the cylindrical pipe

(left: undisturbed inflow, right: disturbed inflow)

Flow Measurement downstream the annular diffuser

The configuration can be split in two kinds of diffusers, an annular diffuser and a dump diffuser (end of hub). Considering ideal pressure conversion the maximum theoretical pressure coefficient can be calculated.

$$c_{p,ideal} = \frac{p_{s,i} - p_{s,1}}{p_{dyn,1}} = 1 - \frac{1}{AR^2} \qquad (9)$$

In order to get a more realistic estimation of the pressure recovery, the recovery mechanisms of this configuration are separately analysed. The recovery coefficient cp is divided into three components:

$$cp = cp_1 + cp_2 + cp_{profile} \qquad (10)$$

where:
cp_1 is pressure recovery of the annular diffuser
cp_2 is pressure recovery of the dump diffuser
$cp_{profile}$ is pressure recovery due to homogenisation of the velocity profile downstream the hub

There are various studies on pressure recovery cp_1 in annular diffusers [1, 2, 4]. The design chart of Sovran and Klomp [1] gives a pressure recovery coefficient, however there is no influence of profile development or profile distortion considered. A more realistic estimation is given by Japikse [5]. The correlation of Japikse takes the area ratio of the diffuser (AR) and an inlet blockage (B) into account.

$$cp = cp_{ideal}\eta(AR)\eta(B) \qquad (11)$$

The pressure recovery cp_2 of the dump diffuser is calculated according to Carnot formula:

$$cp_2 = \frac{p_5 - p_4}{\frac{\rho}{2} c_{1,ax}^2} = 2 \frac{A_1^2}{A_4 A_5} \left(1 - \frac{A_4}{A_5} \right) \tag{12}$$

The outflow profile of the annular diffuser is distorted and inhomogeneous, downstream the hub the flow profile homogenises (Figure 12, Figure 13). This effect causes a static pressure rise, which can be calculated according to following formula:

$$cp_{profile} = \left(\frac{A_1}{A_4} \right)^2 D_4 - \left(\frac{A_1}{A_i} \right)^2 D_i \tag{13}$$

At measurement plane 4 (diffuser outlet) a pressure recovery coefficient cp of 0.54 (undisturbed inflow) and 0.43 (disturbed inflow) is measured (Figure 16). This result reflects the influence of the increased inlet blockage B of the configuration with disturbed inflow. Japikse's correlation for annular diffuser performance takes the inlet blockage B into account and gives results which are close to the experiments ($cp_{MP4, disturbed\ Profile} = 0.52$, $cp_{MP4, undisturbed\ Profile} = 0.44$). Downstream the annular diffuser two pressure recovery mechanisms are combined, the dump diffuser cp_2 and the pressure recovery due to the homogenisation of the profile $cp_{Profile}$. The pressure recovery of the dump diffuser is dependent on the geometry, for this configuration $cp_2 = 0.072$. The reduction of the profile distortion leads to a static pressure recovery $cp_{Profile, disturbed\ inflow} = 0.031$ respectively $cp_{Profile, undisturbed\ inflow} = 0.021$ at MP7. In sum a pressure recovery for the undisturbed configuration $cp_{undisturbed\ inflow} = 0.61$ and $cp_{disturbed\ inflow} = 0.54$ is calculated. These results are in good agreement with the measurement of the static pressure rise in the configuration $cp_{exp, undisturbed\ inflow} = 0.60$ and $cp_{exp, disturbed\ inflow} = 0.55$).
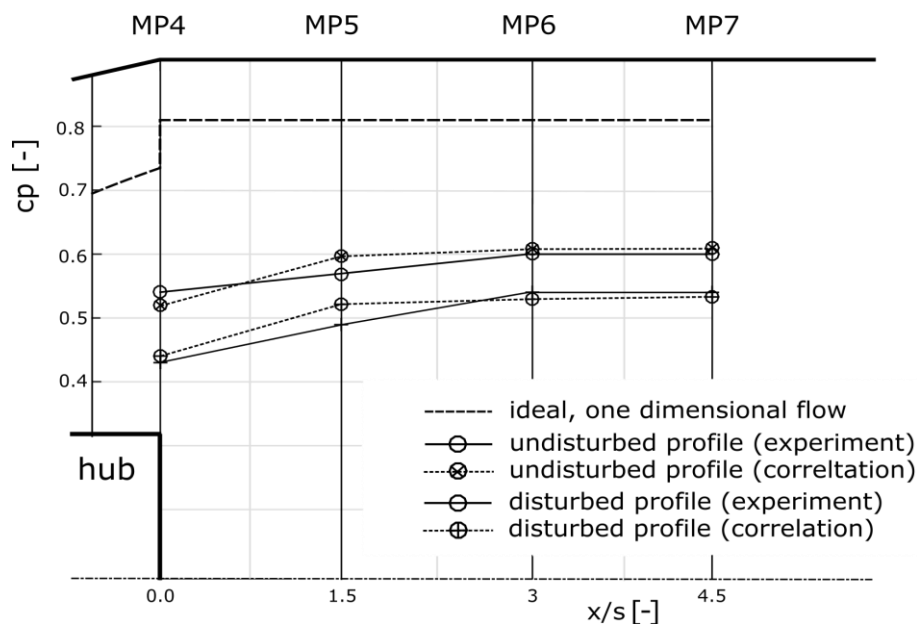
Figure 15. Static pressure recovery of the configuration (experiment and correlation)

Flow Measurement downstream the annular diffuser

The flow characteristic in the diffuser strongly depends on the inlet profile. While the undisturbed profile leads to a stable forward flow at the hub, the typical fan outflow profile (disturbed profile) shows low wall shear stress and thus tendency to separate at the hub. The pressure recovery of the annular diffuser is influenced by the inflow profile. The correlation of Japikse could be proved by the measurements. Downstream the annular diffuser a further pressure rise is caused by the sudden enlargement of the area (dump diffuser) and the homogenization of the velocity profile in the cylindrical pipe. The wake area downstream the hub is filled up and the velocity peaks at the diffuser outflow are damped in the cylindrical pipe section. The pressure recovery for the entire configuration with undisturbed inflow is 60% in MP7. The disturbed inflow configuration "disturbed inflow" converts 55% of dynamic pressure into static pressure at MP7.

Nomenclature

a – speed of sound in air, [ms^{-1}]
A – cross section, [m^2]
AR – area ratio, [–]
A^+ – damping parameter, [–]
B – aerodynamic blockage, [–]
c – flow velocity, [ms^{-1}]
cp – pressure recovery, [–]
D – flow distortion parameter, [–]
D_H – hydraulic diameter, [m]
L   – diffuser length, [m]
p^+ – nondimensional pressure increase, [–]
p_{dyn} – dynamic pressure, [Pa]
p_s – static pressure, [Pa]
r – radial coordinate, [m]
r_H – radius of the hub, [m]
R – radius of the cylindrical pipe, [m]
Ma   – Mach number (= v/a), [–]

Re   – Reynolds number (= $D_H·c/v$), [–]
s – annular gap height at diffuser inlet, [m]
s_i – annular gap position (= r-r$_H$), [–]
Tu   – turbulence intensity, [%]
u_τ – friction velocity, [ms^{-1}]
x – coordinate, [m]

Greek symbols

κ – Von Kármán constant, [–]
v – kinematic viscosity, [m^{2}s^{-1}]

References

[1] Sovran, G., Klomp, E. D., Experimentally determined optimum geometries for rectilinear diffusers with rectangular, conical or annular cross-section (Optimum geometry for rectilinear diffuser with rectangular, conical or annular cross section noting flow regime, performance characteristics and boundary layer effect), *Fluid mechanics of internal flow*, *20* (1967), 21, pp. 270-319
[2] Stevens, S. J., Williams, G. J., The influence of inlet conditions on the performance of annular diffusers, *Journal of Fluids Engineering*, *102* (1980), 3, pp. 357-363
[3] Dierksen, J. M., A Study of Annular Diffuser Flow Using A Photon-Correlating Laser Doppler Anemometer, Airforce Inst Of Tech Wright-Patterson AFB OH School Of Engineering, 1983
[4] Traupel, W., *Thermische Turbomaschinen: Erster Band Thermodynamisch-strömungstechnische Berechnung*, Springer-Verlag, Berlin, 2013

[5] Japikse, D.., Correlation of annular diffuser performance with geometry, swirl, and blockage, *Proceedings of the 11th NASA/OSU Thermal and Fluids Analysis Workshop*, 10th World Energy Conference, Cleveland, USA, 2002, pp. 107-118

[6] Walter, W., *Strömungsmeßtechnik: Lehrbuch für Aerodynamiker, Strömungsmaschinenbauer Lüftungs- und Verfahrenstechniker ab 5. Semester*, Springer-Verlag, Berlin, 2013

[7] Nitsche, W., *et al*., A computational Preston tube method, *Turbulent Shear Flows*, *4* (1985), 3, pp. 261-276

[8] Cherry, E. M., *et al*., Three-dimensional velocity measurements in annular diffuser segments including the effects of upstream strut wakes, *International Journal of Heat and Fluid Flow*, *31* (2010), 4, pp. 569-575

[9] Cebeci, T., *et al*., Calculation of separation points in incompressible turbulent flows, *Journal of Aircraft*, *9* (2010), 9, pp. 618-624

[10] Schlichting, H., *Boundary Layer Theory*, Springer-Verlag, Berlin, 1987